Correlations between density distributions, optical spectra, and ion species in a hydrogen plasma (invited)

O. D. Cortázar,[1,a)] A. Megía-Macías,[2,b)] O. Tarvainen,[3] T. Kalvas,[3] and H. Koivisto[3]
[1]*INEI-Institute for Energy Research, University of Castilla-La Mancha, Camilo José Cela s/n, 13170 Ciudad Real, Spain*
[2]*ESS Bilbao Consortium, Polígono Ugaldeguren-III Pol. A 7B, 48170 Zamudio, Vizcaya, Spain*
[3]*Department of Physics, University of Jyväskylä, PO Box 35 (YFL), 40500 Jyväskylä, Finland*

(Presented 28 August 2015; received 18 August 2015; accepted 12 September 2015; published online 1 October 2015)

An experimental study of plasma distributions in a 2.45 GHz hydrogen discharge operated at 100 Hz repetition rate is presented. Ultrafast photography, time integrated visible light emission spectra, time resolved Balmer-alpha emission, time resolved Fulcher Band emission, ion species mass spectra, and time resolved ion species fraction measurements have been implemented as diagnostic tools in a broad range of plasma conditions. Results of plasma distributions and optical emissions correlated with H^+, H_2^+, and H_3^+ ion currents by using a Wien filter system with optical observation capability are reported. The magnetic field distribution and strength is found as the most critical factor for transitions between different plasma patterns and ion populations. © *2015 AIP Publishing LLC.* [http://dx.doi.org/10.1063/1.4931720]

I. INTRODUCTION

Hydrogen discharges at 2.45 GHz are one of the most popular plasmas for ion sources in a wide range of application fields from accelerators to industry.[1–3] Recent results demonstrate the capabilities of 2.45 GHz plasma sources for producing intense beams of molecular hydrogen ions[4,5] attracting the interest on these devices for manifold applications.[6,7] Several plasma distributions where visible light emission suggests different dynamics of the H^+, H_2^+, and H_3^+ populations have been reported.[8,9] Thus, visible light spectroscopy has been recently proposed as a non-invasive qualitative diagnostic for monitoring the plasma species fraction during ion source operation in a 2.45 GHz hydrogen plasma discharge.[10] We report herein a study of the H^+, H_2^+, and H_3^+ current correlated with visible filtered, Balmer-α and Fulcher band emissions, and plasma distributions recently observed.

II. EXPERIMENTAL SETUP

The plasma source dimensions and characteristics have been presented in Ref. 11. An extraction electrode system and a Wien filter ion velocity analyzer with optical measurement capability have been used to perform the study. Figure 1 shows a half-section view of the experiment where the most important blocks can be seen: *Plasma source + extraction, Wien filter, and Faraday's cup*. Note the axial line of sight along the axis of the system. The characteristics and performance of the setup are described in detail in Ref. 10. The system can extract currents in the order of 1 mA analyzing the beam in two acquisition modes: *spectrum* or *ion species evolution*. In the *spectrum* mode, the Wien filter can obtain spectra of (singly charged) ion mass in a range between 1 and 20 amu. This operation mode is designed to be used by obtaining data from different consecutive pulses. The timing for the data acquisition must be specified. Once the spectrum is obtained and the ion species are identified, the voltages corresponding to each species can be used in the *ion species evolution* mode. In this mode, the system can acquire *current vs. time* signals for selected voltages allowing to obtain the temporal response of each ion species with 1 μs resolution. The *plasma electrode, extraction system, and Wien filter* were designed using the *IBSimu* code.[12]

III. RESULTS

A comprehensive study of the H^+, H_2^+, and H_3^+ spectra and currents correlated with visible (390-700 nm), Balmer-α

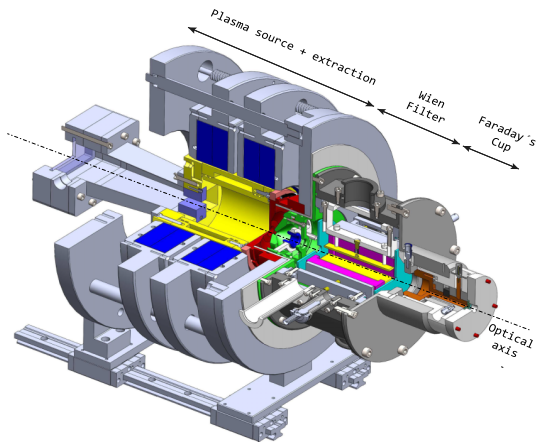

FIG. 1. Half-section of the experiment where the most important blocks can be seen: *Plasma source + extraction, Wien filter, and Faraday's cup*.

Note: Invited paper, published as part of the Proceedings of the 16th International Conference on Ion Sources, New York, New York, USA, August 2015.

a)Author to whom correspondence should be addressed. Electronic mail: daniel.cortazar@uclm.es
b)Present address: CERN, BE-ABP-HSL Department, CH1211 Geneva, Switzerland.

 © 2015 AIP Publishing LLC
This article is copyrighted as indicated in the article. Reuse of AIP content is subject to the terms at: http://scitationnew.aip.org/termsconditions. Downloaded to IP: 161.67.111.30 On: Thu, 01 Oct 2015 13:47:22

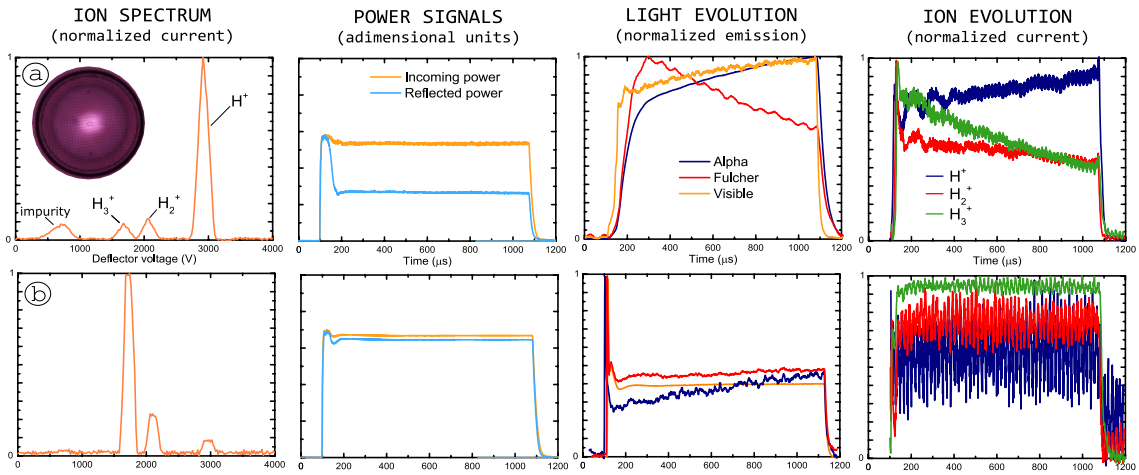

FIG. 2. Data arrangement for the two sets of plasma parameters where *Column* distribution is observed. Case (a): 3.8×10^{-3} mbar of pressure and 1500 W of incoming power. Case (b): 8.5×10^{-3} mbar of pressure and 2100 W of incoming power.

(486.1 nm), and Fulcher band emission (around 600 nm) was conducted. The Balmer-α and Fulcher band signals were obtained using band pass filters (Thorlabs models FB488-10 with 488 nm central wavelength and 10 nm bandpass region and FB600-40 with 600 nm central wavelength and 40 nm bandpass region) and a photomultiplier tube. The study was carried out covering the full range of operation parameters where stable plasma distributions (*Column, Hourglass, Slug, Fullchamber, Ring, Flower, YinYang, and Donut*) are created and mainly determined by the magnetic field profile as previously reported.[8,9] Pictures obtained with a regular camera are included in the following figures to facilitate the association with the corresponding plasma distributions. Incoming and reflected microwave powers were also measured to include the coupling characteristics.

Figure 2 shows a data arrangement for the two most significant parameter sets resulting to *Column* plasma distributions. Each row shows the ion spectrum obtained at the middle of the pulse (steady state stage), the coupling evolution by incoming and reflected power signals, the temporal evolution of light signals for visible, Balmer-α, and Fulcher band, and the normalized temporal evolution of ion species currents for H^+, H_2^+, and H_3^+. Case (a) corresponds to a high intensity light emission with a reasonable power coupling factor of 50% and (b) to a poor intensity case with a low coupling of 5%. In case (a), the H^+ is predominant but H_3^+ is the most intense ion current for the case (b). Moreover, the H^+ current and Balmer-α signals show both similar temporal profiles and the molecular currents (H_2^+ and H_3^+) follow the temporal behavior of Fulcher band emission even during the breakdown transient. For the case (a), Balmer-α shows a continuous increase while Fulcher band emission exhibits the inverse behavior with a fast increase during breakdown followed by a slow decay. For case (b), the Fulcher band signal follows the H_3^+ current evolution remaining constant during the entire pulse length while Balmer-α signal grows only slowly.

Figure 3 shows a similar data arrangement for the *Hourglass* plasma distribution. The predominance of H^+ production is shown with coupling factors of about 40%-45%. The similarity of optical signals respect to ion currents is remarkable even during the transients.

Figure 4 shows data for the *Slug* plasma distribution. Although both cases present a H^+ predominance, (a) has a coupling factor of 70% while (b) barely reaches 10%. The inversion of ratio between H_2^+ and H_3^+ and the considerable breakdown transient peak (in both light and current signals) for case (b) respect to (a) could be related to the coupling characteristics. The breakdown times and couplings suggest different ionization dynamics between for each case. However, the connection between ion currents and light signals is remarkable even during the breakdown transients.

Figure 5 shows data from the *Fullchamber* plasma distribution. It presents a H^+ predominance with coupling factor around 50%. The follow-up between ion currents and light signals is again observable with exception of the fast pulse

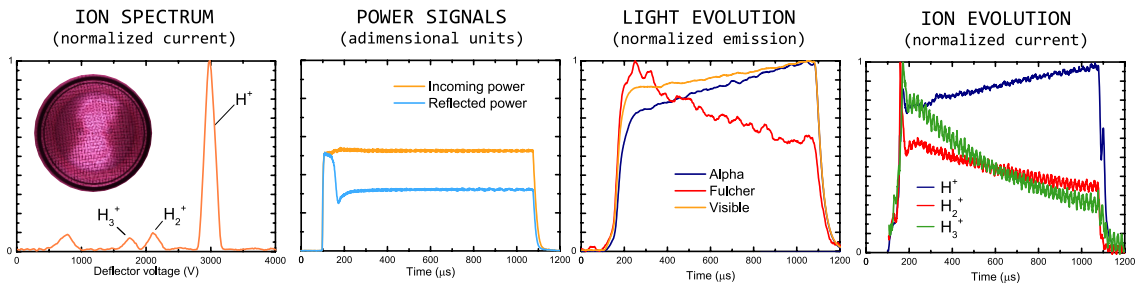

FIG. 3. Data arrangement for the set of plasma parameters where *Hourglass* distribution is observed: 3.8×10^{-3} mbar of pressure and 1500 W of incoming power.

This article is copyrighted as indicated in the article. Reuse of AIP content is subject to the terms at: http://scitationnew.aip.org/termsconditions. Downloaded to IP: 161.67.111.30 On: Thu, 01 Oct 2015 13:47:22

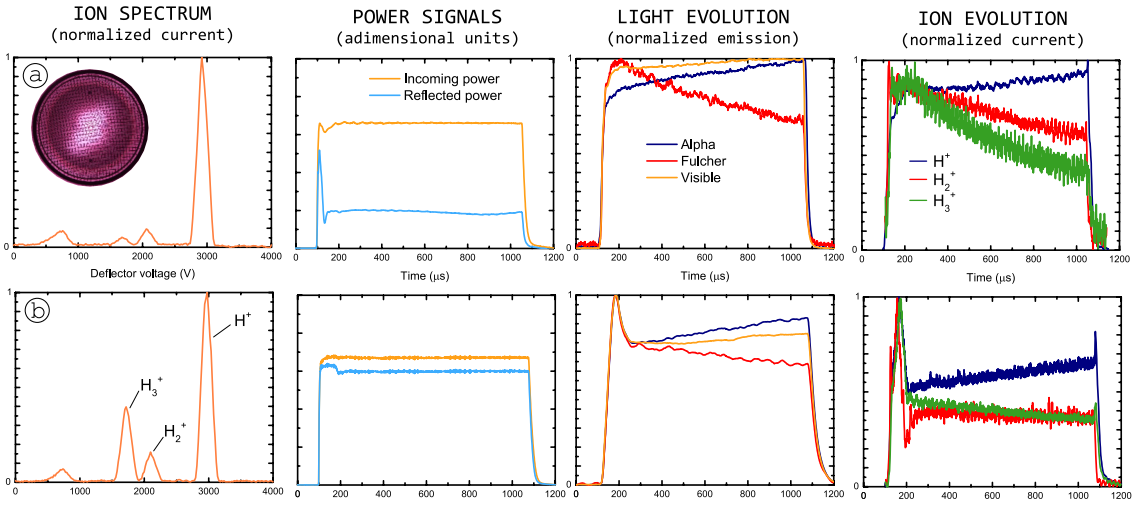

FIG. 4. Data arrangement for the two sets of plasma parameters where *Slug* distribution is observed. Case (a): 3.8×10^{-3} mbar of pressure and 600 W of incoming power. Case (b): 6.9×10^{-3} mbar of pressure and 1500 W of incoming power.

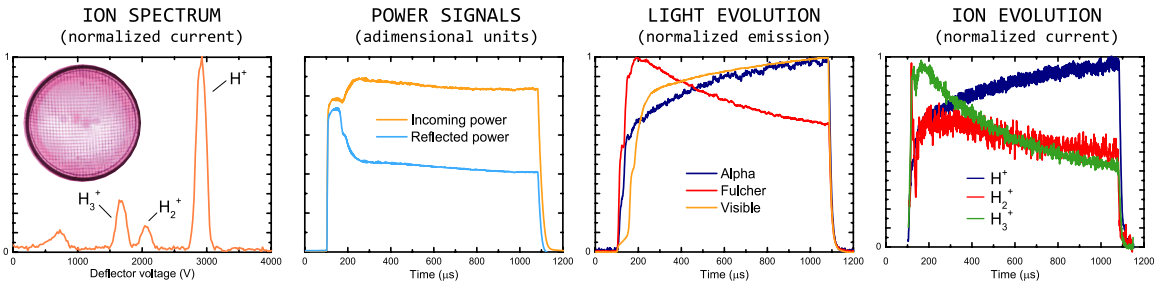

FIG. 5. Data arrangement for the set of plasma parameters where *Fullchamber* distribution is observed: 3.8×10^{-3} mbar of pressure and 2550 W of incoming power.

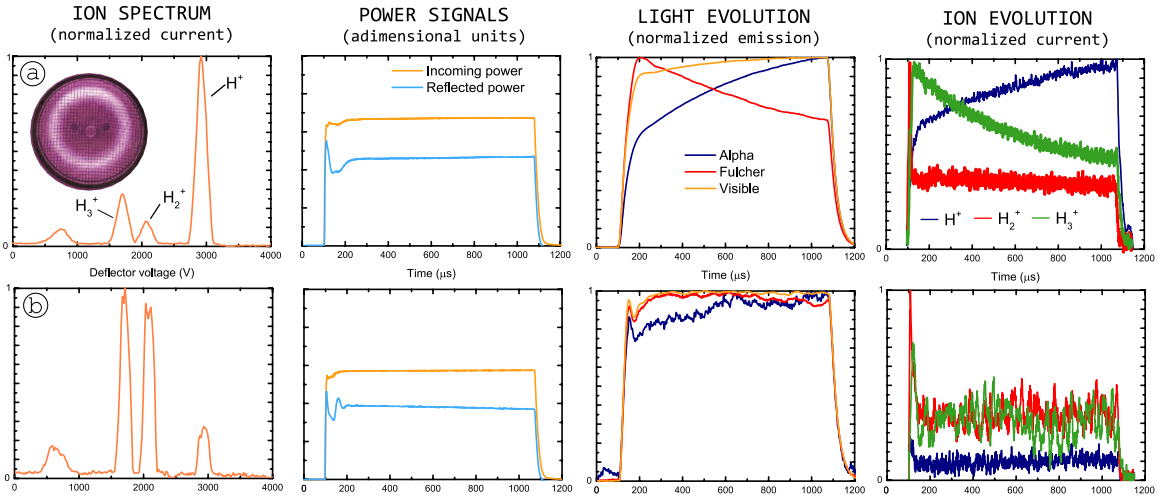

FIG. 6. Data arrangement for the two sets of plasma parameters where *Ring* distribution is observed. Case (a): 6.9×10^{-3} mbar of pressure and 1500 W of incoming power. Case (b): 3.8×10^{-3} mbar of pressure and 1350 W of incoming power.

(less than 20 μs) during the breakdown for the H_2^+ current that is not reflected in the Fulcher band signal.

Figure 6 shows data from the *Ring* plasma distribution. Although coupling factors of 40% are similar for both cases, the ratios of ion currents appear to be quite different. While the spectrum of case (a) presents a typical dominance of H^+, the production of H_2^+ and H_3^+ is remarkably higher than H^+ for the case (b). Other noticeable difference is the temporal behavior of ion currents, where a remarkable peak of H_2^+ and H_3^+ is produced during the first 20 μs of the breakdown process remaining practically constant after that. Otherwise, the tracing between optical signals and ion currents is good for the case (a) but the short pulse of H_2^+ during the breakdown is not reflected in the Fulcher band signal.

Figure 7 shows data for the *Flower* (a), *YinYang* (b), and *Donut* (c) plasma distributions. Coupling factors reaches

This article is copyrighted as indicated in the article. Reuse of AIP content is subject to the terms at: http://scitationnew.aip.org/termsconditions. Downloaded to IP: 161.67.111.30 On: Thu, 01 Oct 2015 13:47:22

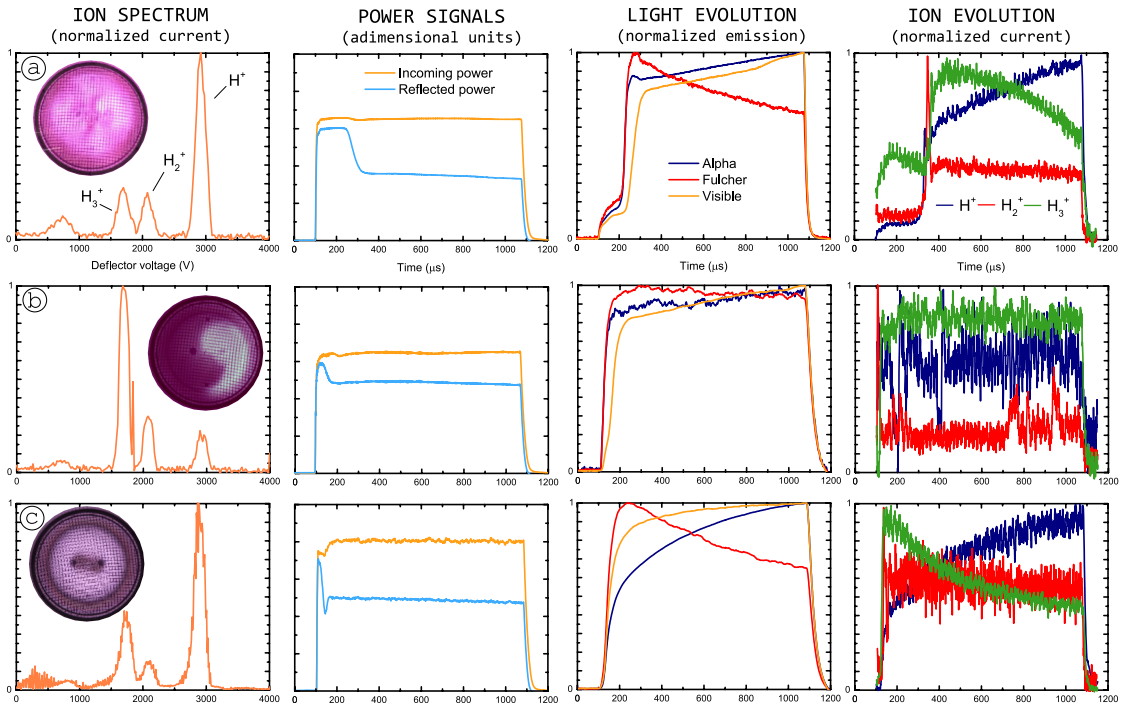

FIG. 7. Data arrangement for the *Flower* (a) 3.8×10^{-3} mbar of pressure and 1500 W of incoming power, *YinYang* (b) 4.9×10^{-3} mbar of pressure and 1200 W of incoming power, and *Donut* (c) 9.6×10^{-3} mbar of pressure and 2100 W of incoming power.

TABLE I. Maximum of species current values recorded for each plasma distribution during the steady state stage.

Distribution	$H^+(\mu A)$	$H_2^+(\mu A)$	$H_3^+(\mu A)$
Column (a)	140	15	12
Column (b)	2	3	12
Hourglass	130	15	14
Slug (a)	180	18	10
Slug (b)	80	17	38
Fullchamber	80	10	20
Ring (a)	60	7	17
Ring (b)	2.5	6	7
Flower	50	12	13
YinYang	3	3.5	10
Donut	55	5.5	24

45%, 25%, and 50%, respectively, where breakdown shows remarkable differences. Note the good correlation between optical signals and ion species currents and the spectacular predominance of H_3^+ line for the *YinYang* (b) case. However, fast pulses of H_2^+ at very beginning of breakdown are not resolved by optical signals as is clear for cases (a) and (b). It is also noticeable the long time required for breakdown in the case (a) where almost 400 μs are recorded in contrast with 50-80 μs for the other cases. Table I shows the peak values of the ion species currents obtained during the steady state stage corresponding to ion spectra of figures.

IV. DISCUSSION

The experiments reveal a strong temporal correlation between ion species and optical emissions as has been proposed by the authors in previous works.[9,10] The measurements clearly show that Balmer-α emission could be used as a representative signal of proton population in the plasma and the Fulcher band signal as a representative indication of molecular H_2^+ and H_3^+ ions' production. Moreover, the influence of the plasma distributions on the current species and its ratios is also demonstrated.

On the other hand, these results help to complete previous studies of Balmer-α and Fulcher band spatial distributions during plasma transients and steady-state stages[8,9] that show how the molecular dissociation and atom excitation dynamics take place in time and space. An interesting example is the case of *Column* configuration shown in Fig. 2(b) where a low microwave coupling under a low gradient of magnetic field with a half-resonance ($B_{ECR}/2$) surface practically placed in the middle of the plasma chamber[8] produces a remarkable ratio inversion with relative high H_3^+ production. In addition, *Ring* and *YingYang* distributions show in Figs. 6(b) and 7(b) also inverted ratios where molecular ions dominate the spectra under a magnetic field topology completely out of resonance[8] (with typical values around 60 mT) and low light intensity emission. Taking into account that the measurements were carried out on the axis and the plasma distributions for the late cases have pronounced radial profiles, the results suggest also unsuspected ion species radial distributions.

Moreover, are also noticeable the peaks of ion production during the breakdown process where H_2^+ is remarkable for *Column* in Fig. 2(b), *Hourglass* in Fig. 3, *Slug* in Fig. 4(b), *Fullchamber* in Fig. 5, *Ring* in Figs. 6(a) and 6(b), *Flower* in Fig. 7(b), and *YinYang* in Fig. 7(c). These peaks are variable in duration between 20 and 100 μs and reach currents more than two times higher respect to values shown in Table I.

This article is copyrighted as indicated in the article. Reuse of AIP content is subject to the terms at: http://scitationnew.aip.org/termsconditions. Downloaded to IP: 161.67.111.30 On: Thu, 01 Oct 2015 13:47:22

However, for the range of experimental conditions under study, the data suggest that the inversion of fraction ratios between protons and molecular ions is associated to a drop in the proton production for determined plasma configurations.

Finally, the ion species ratio behaviors reported here open a lot of questions about the temporal and spatial dynamics of the Electron and Ion Energy Distribution Functions (EEDF and IEDFs) during transients and steady-state stages for this kind of plasma. The understanding of such dynamics may lead to some plasma tuning technical approaches for a wide range of applications.

[1]R. Gobin, N. Chauvin, O. Delferrière, T. O., and D. Uriot, in Proceedings of LINAC2012, Tel-Aviv, Israel, 2012.
[2]M. Cao, J. Cheng, C. Han, and L. Ji, Adv. Mater. Res. **1006**, 193 (2014).
[3]J. Pelletier and A. Anders, IEEE Trans. Plasma Sci. **33**, 1944 (2005).
[4]R. Xu, J. Zhao, S. Peng, Z. Yuan, Z. Song, J. Xu, and Z. Guo, Rev. Sci. Instrum. **79**, 02B713 (2008).
[5]Y. Xu, S. Peng, H. Ren, J. Zhao, J. Chen, A. Zhang, T. Zhang, Z. Guo, and J. Chen, Rev. Sci. Instrum. **85**, 02A943 (2014).
[6]R. Gobin, V. Blideanu, D. Bogard, G. Bourdelle, N. Chauvin, O. Delferrière, P. Girardot, J. Jannin, S. Langlois, D. Loiseau, B. Pottin, J.-Y. Rousse, and F. Senée, Rev. Sci. Instrum. **81**, 02B301 (2010).
[7]J. Alonso, W. Barlleta, M. Toups, J. Conrad, Y. Liu, M. Bannister, C. Havener, and R. Vane, Rev. Sci. Instrum. **85**, 02A509 (2014).
[8]O. D. Cortázar, A. Megía-Macías, O. Tarvainen, A. Vizcaíno-de-Julián, and H. Koivisto, Plasma Sources Sci. Technol. **23**, 065028 (2014).
[9]O. Cortázar, A. Megía-Macías, O. Tavainen, and H. Koivisto, Nucl. Instrum. Methods Phys. Res., Sect. A **781**, 50 (2015).
[10]O. Cortázar, A. Megía-Macías, O. Tarvainen, T. Kalvas, and H. Koivisto, Rev. Sci. Instrum. **86**, 083309 (2015).
[11]A. Megía-Macías, O. D. Cortázar, and A. Vizcaíno-de-Julián, Rev. Sci. Instrum. **85**, 033310 (2014).
[12]T. Kalvas, O. Tarvainen, T. Ropponen, O. Steczkiewicz, J. Arje, and H. Clark, Rev. Sci. Instrum. **81**, 02B703 (2010).

This article is copyrighted as indicated in the article. Reuse of AIP content is subject to the terms at: http://scitationnew.aip.org/termsconditions. Downloaded to IP: 161.67.111.30 On: Thu, 01 Oct 2015 13:47:22